J. Electrochem. Sci. Eng. **15(3)** (2025) 2671; http://dx.doi.org/10.5599/jese.2671

Open Access : : ISSN 1847-9286
https://pub.iapchem.org/ojs/index.php/JESE

Original scientific paper

The preferred orientation of electrodeposited dendrites of lead, tin and zinc

Nebojša D. Nikolić[1,✉], Jelena D. Lović[1], Vesna M. Maksimović[2], Nikola S. Vuković[3] and Predrag M. Živković[4]

[1]*Department of Electrochemistry, Institute of Chemistry, Technology and Metallurgy, University of Belgrade, Njegoševa 12, 11000 Belgrade, Serbia*
[2]*Vinča Institute of Nuclear Science—National Institute of the Republic of Serbia, University of Belgrade, 11000 Belgrade, Serbia*
[3]*Institute for Technology of Nuclear and Other Mineral Raw Materials, Bulevar Franše d'Eperea 86, 11000 Belgrade, Serbia*
[4]*Faculty of Technology and Metallurgy, University of Belgrade, Karnegijeva 4, 11000 Belgrade, Serbia*

Corresponding author: ✉nnikolic@ihtm.bg.ac.rs;Tel.: +381-11-337-03-90; Fax: +381-11-337-03-89

Received: February 11, 2025; Accepted: March 6, 2025; Published: March 8, 2025

Abstract

Morphology and crystal orientation of electrolytically produced dendrites of lead, tin, and zinc have been investigated with the aim of establishing any correlation between them. These three metals belong to the same group of metals from an electrochemical point of view (the group of normal metals), but to various types of crystal lattice (Pb - the face-centered cubic type, Sn - the body-centered tetragonal type, and Zn - the hexagonal closed pack type). Pb, Sn and Zn dendrites were produced potentiostatically using the corresponding hydroxide electrolytes and characterized by scanning electron microscopy (morphology) and X-ray diffraction (crystal orientation) techniques. The preferred orientation of the dendritic particles was determined by applying a method based on a comparison of the peak intensity ratios. The fern-like dendrites of various degrees of branchy were obtained by the processes of electrolysis, and regardless of the type of crystal lattice, they exhibited the strong preferred orientation in crystal planes with the lowest surface energy. Based on the performed analysis, a strong correlation between the morphology and the crystal structure of dendrites belonging to the group of normal metals has been established. It is concluded that electrochemical parameters characterized by the high values of the exchange current density (the fast electrochemical processes) prevailed over crystallographic characteristics of metals manifested by the belonging to a determined type of crystal lattice.

Keywords

Electrolysis; morphology; crystal orientation; scanning electron microscopy, X-ray diffraction

Introduction

Metal powders consist of particles that are the smallest unit of a powder, and they can be obtained by various production techniques, such as solid-state reduction, atomization, electrolysis, and chemical processes [1,2]. Among all techniques, electrolysis has emerged as a technique offering numerous advantages over the other techniques. The high purity of synthesized powders, easy control of the shape and size of powder particles, relatively low price, and environmentally friendly powder production are only some of the advantages of electrolysis as a production technique [3,4]. Although electrolysis from aqueous electrolytes is the most common procedure for powder production of all technologically important metals [1,5,6], the electrolytic processes from non-aqueous electrolytes [7,8], deep eutectic solvent (DES) [9-12], melt [13,14] and ionic liquids [15] have recently attracted significant attention.

The dendrites represent the most significant form of powder particles synthesized via various electrodeposition routes from aqueous electrolytes [1,5,6,16-26]. The particles resembling flakes, fibrous, wires, needles, mossy as well as cauliflower and spongy formed under strong hydrogen evolution as a parallel reaction during metal electrolysis are some of the powder forms which can also be obtained by the electrolysis processes [5,6,24,27-32]. The powder particles are obtained by the removal of a deposit from the cathode surface after the finished electrolysis process in some suitable way [1]. Aside from the particles formed in the conditions of vigorous hydrogen evolution (cauliflower and spongy), the other types of particles are obtained in the diffusion-controlled electrodeposition process.

The main parameters of electrolysis that affect the shape and size of the powder particles are the type and composition of electrolysis solution, the temperature, a kind of cathodic material, the solution stirring, the electrolysis time, an addition of specific substances in a solution, hydrogen evolution reaction as a parallel reaction, *etc.* [1,33]. Both constant regimes of electrolysis are used for the production of metal powders, and the desired morphology of the particles is realized by the choice of current density or cathodic potential (overpotential). Modelling the shape of the particles can also be realized by the application of periodically changing regimes of electrolysis, such as the pulsating overpotential (PO), the pulsating current (PC) and the reversing current (RC) [1,34-36].

However, the nature of metals is the largest influence on the shape of dendrites and on the kind of other powder particles that can be formed via the electrolytic route. Following electrochemical parameters, such as the exchange current density (i_0), melting point (T_m) and an overpotential for hydrogen evolution reaction (η (H_2)), metals can be located in one of the following groups [37]:

a) the normal metals (Pb, Ag (basic electrolyte), Zn, Sn and Cd): this group of metals is featured by: high i_0 ($i_0 > 1$ A dm^{-2}), high η (H_2), and low T_m,
b) the intermediate metals (Cu, Au, Ag (complex electrolyte)): this group of metals is featured by: medium i_0 ($10^{-2} < i_0 < 1$ A dm^{-2}), moderate T_m, and η (H_2) lower than those characterizing the normal metals, and
c) the inert metals (Fe, Co, Ni, Mn, Cr, Pt): this group of metals is featured by low i_0 ($10^{-2} < i_0 < < 10^{-12}$ A dm^{-2}), high T_m and very low η (H_2).

Simultaneously, metals electrocrystallize in different types of crystal lattices, and the main crystal lattices in which electrocrystallization of technologically important metals occur are face-centered cubic (Pb, Ag, Au, Ni, Cu, Co), body-centered tetragonal (Sn) and hexagonal closed pack (Zn) types [38].

Taking into consideration the morphological characteristics of the electrolytically produced powder particles and their preferred orientation obtained for typical representatives of metals that belong to the face-centered cubic type of crystal lattice, such as Pb, Ag, Cu and Ni, the strong correlation between these two characteristics of the particles was recently established [6]. The

(cc) BY

change of the preferred orientation from the strong (111) obtained for the needles and the 2D fern-like dendrites to the random orientation obtained for the particles with spherical grains as a constitutive element (the 3D pine-like dendrites, cauliflower and spongy) was observed with the decrease of the exchange current density. To complete an insight into the correlation between the morphology and the preferred orientation of powder particles, it was necessary to examine other types of crystal lattice besides the face-centered cubic lattice. For that reason, this study aimed to compare the morphological and structural characteristics of three metals (Pb, Sn and Zn) belonging to the same group of metals from an electrochemical point of view (a group of normal metals) but to the different types of crystal lattice.

Experimental

Electrodeposition of lead, tin and zinc in dendrites was performed by potentiostatic regime of electrolysis at room temperature using potentiostat/galvanostat BioLogic SP 200. All electrodepositions were performed on copper as the working electrode (WE).

Pb was electrodeposited from an electrolyte containing 0.10 M $Pb(NO_3)_2$ in 2.0 M NaOH at an overpotential of -90 mV *vs.* Pb with an electrodeposited charge of 0.50 mAh. The electrodeposition time was 110 s. The counter and the reference electrodes were of lead.

Sn was electrodeposited from an electrolyte containing 0.090 M $SnCl_2$ in 6.25 M NaOH at a cathodic potential of -1400 mV *vs.* Ag/AgCl with an electrodeposited charge of 0.11 mAh. The electrodeposition time was 330 s. The counter electrode was Pt, while Ag/AgCl/3.5 M KCl was used as the reference electrode.

Zn was electrodeposited from an electrolyte containing 0.35 M ZnO in 6.0 M KOH at over-potentials of -220 and -280 mV *vs.* Zn with an electrodeposited charge of 1.5 mAh. For this electro-deposited charge, the times of electrodeposition were 350 s at -220 and 242 s at -280 mV *vs.* Zn. The counter and the reference electrodes were of zinc.

The electrolytes were made of double distilled water and analytical grade chemicals, and all electrodepositions were performed in cells of an open type. Copper working electrodes were cylindrical with surface areas of 1.0 cm^2 for Pb, 0.25 cm^2 for Sn and 0.50 cm^2 for Zn electrodeposition processes. The different sizes of Cu WE did not affect the valuability of the obtained results. The following procedure was applied for the preparation of Cu WE: (I) degreasing in alkaline detergent at a temperature of 70 °C for a duration of 120 s, (II) rinsing in the distilled water, (III) etching in 20 % H_2SO_4 at a temperature of 50 °C in a duration of 60 s and (IV) rinsing in the distilled water.

Morphology of dendritic particles of Pb, Sn and Zn was characterized by scanning electron microscopy (SEM) technique, using the following models of a microscope: TESCAN Digital Micro-scopy for Pb, JEOL JSM-6610LV for Sn, and JEOL JSM-7001F for Zn. The particles were characterized without or with their removal from the Cu WE after the electrolysis processes.

The structure of the dendritic particles was examined using the X-ray diffraction (XRD) method using Rigaku Ultima IV diffractometer with CuKα radiation. The examined 2θ ranges were between 30 and 80° for Pb and Zn, and between 20 and 100° for Sn. For this kind of analysis, the particles were removed from the Cu WE and analyzed in powder form.

Results and discussion

For easier analysis, the same type of electrolyte (a hydroxide electrolyte) was used for the electrolytic production of dendrites. Also, before a detailed analysis of the shape of dendrites, some basic information related to this term must be given. The term “dendrite” originates from the Greek

word *dendron,* which means tree [39,40]. According to Wranglen [41], a dendrite consists of a trunk and branches. The branches developed from a trunk are referred to as primary (P) branches, while those developed from the primary branches are known as the secondary (S) branches. The tertiary (T) branches are developed from the secondary branches. If a trunk and branches are in the same plane, a dendrite is a 2D (two-dimensional) dendrite.

Morphology of Pb, Sn and Zn dendrites electrodeposited from the hydroxide electrolytes

Figure 1 shows the morphology of Pb dendrites obtained at an overpotential of -90 mV *vs.* Pb (Figures 1a and 1b), Sn dendrites obtained at a cathodic potential of -1400 mV *vs.* Ag/AgCl (Figure 1c and 1d), and Zn dendrites obtained at an overpotential of -220 mV *vs*. Zn (Figure 1e and 1f) from the corresponding hydroxide electrolytes.

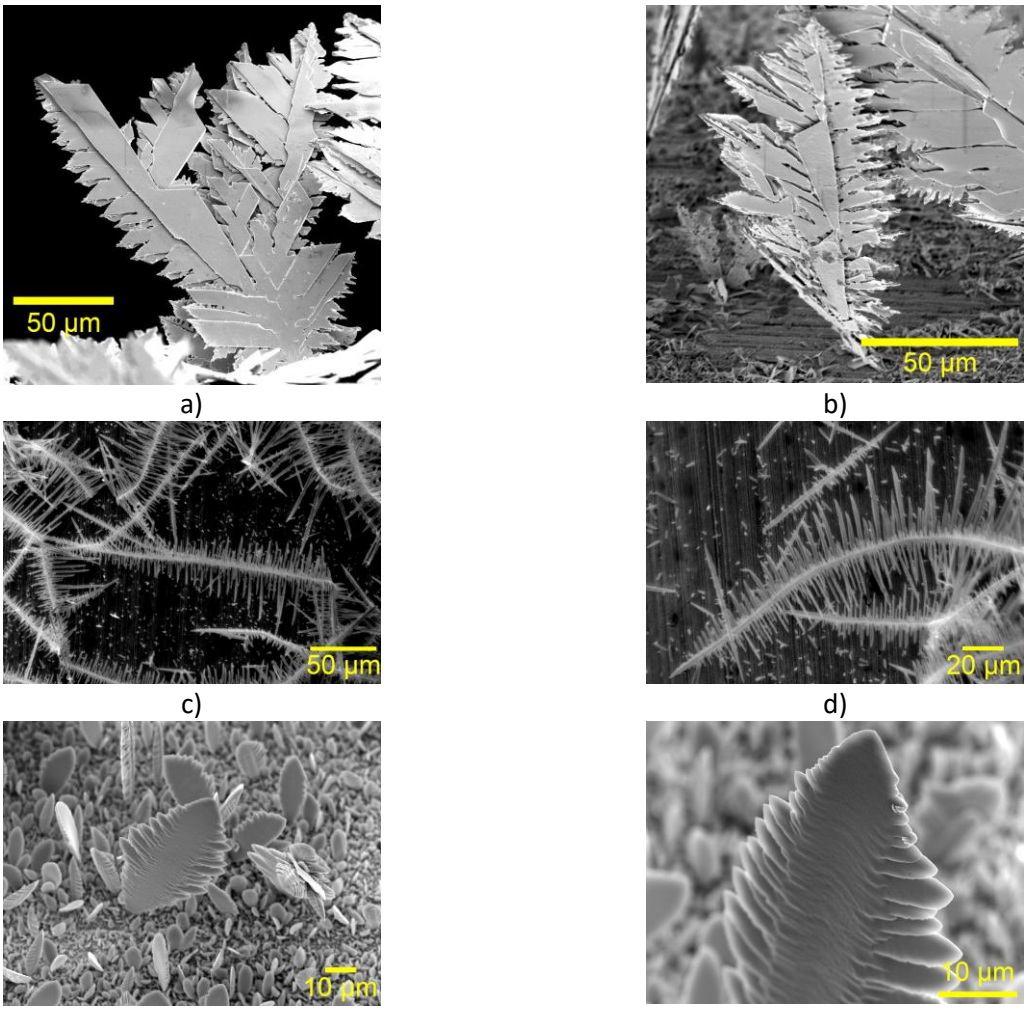

Figure 1. *The dendrites of: (a) and (b) Pb obtained by electrolysis at an overpotential of -90 mV vs. Pb [31], (c) and (d) Sn obtained by electrolysis at a cathodic potential of -1400 mV vs. Ag/AgCl, and (e) and (f) Zn obtained by electrolysis at an overpotential of -220 mV vs. Zn*

The very branchy 2D (two-dimensional) dendrites of the fern-like shape with clearly noticeable primary, secondary and tertiary branches were produced by the Pb electrolysis (Figure 1a and 1b). The dendrites of Sn are also 2D with a fern-like shape but not so branchy as Pb dendrites (Figure 1c and 1d). Sn dendrites were built from a trunk, and primary branches developed under the right angle from the trunk. The other types of branches from this electrolyte did not develop during Sn

(cc) BY

electrolysis. The 2D fern-like dendrites constructed from stalk and primary branches were formed under given conditions of Zn electrolysis (Figure 1e and 1f).

At first sight, it can be noticed that the 2D fern-like dendrites of Pb had a more branchy morphology than Sn and Zn dendrites. It is necessary to note that although there are differences at the macro level, all are 2D and have fern-like shapes. The differences among them can be attributed to the specificity of every metal and the type of electrolyte used for its production. Namely, the 2D Pb fern-like dendrites built of a trunk and primary branches are obtained by electrolysis from the nitrate electrolyte, while the 2D Pb fern-like dendrites built of a trunk, primary and secondary branches were obtained by an electrolysis from the acetate electrolyte [6].

The crystal orientation of electrodeposited dendrites of Pb, Sn and Zn

Figure 2 shows the XRD patterns together with corresponding standards for the electrolytically produced particles of lead (Figures 2a and 2b), tin (Figures 2c and 2d) and zinc (Figures 2e and 2f). The diffraction peaks were only observed at the angles corresponding to those of the standards, clearly pointing out that the high purity of produced powder particles of Pb, Sn and Zn was obtained. From the obtained diffractograms, it is clearly visible that crystallites of Pb were predominately oriented in the (111), Sn in (220) and Zn in (002) crystal planes. On the other hand, the appearance of obtained diffractograms strongly differed from those predicted by the standards for these metals, which definitely indicates the existence of the preferred orientation in the dendritic particles of Pb, Sn and Zn.

A procedure based on a comparison of the peak intensity ratios was applied to estimate the preferred orientation of the particles. This procedure predicts a comparison of the peak intensity ratios made relative to the peak with the maximum intensity with the same ratios for the standard [18,29,42]. It is the fastest method for an estimation of the preferred orientation and can be explained as follows: the larger peak intensity ratios than those predicted by the standards mean the existence of the preferred orientation in a crystal plane with the maximum intensity of the diffraction peak. If the values of the peak intensity ratios are comparable with those of the standards, then the particles are randomly oriented. Finally, the values of the peak intensity ratios smaller than those for the standard point out the preferred orientation in a crystal plane with the smaller intensity of the diffraction peak than that having the maximum intensity.

The calculated values of the peak intensity ratios for the particles of Pb, Sn and Zn and those for the standards are given in Table 1. Analysis of the obtained ratios showed that the particles of Pb showed (111)(222), the particles of Sn (220)(440) and the particles of Zn (002)(004) preferred orientations.

The common characteristic of the preferred orientation in these crystal planes is that they have the lowest surface energy in the corresponding type of crystal lattice [43-46]. During an electrolysis process, they survive a process of growth, constructing both trunk and branches in the dendrites [47]. All other crystal planes have higher surface energies and disappear during growth. It is the reason for the considerably smaller intensities of the diffraction peaks of these crystal planes than those predicted by the standards. The tips and the angles of the dendrites are built of crystallites oriented in them.

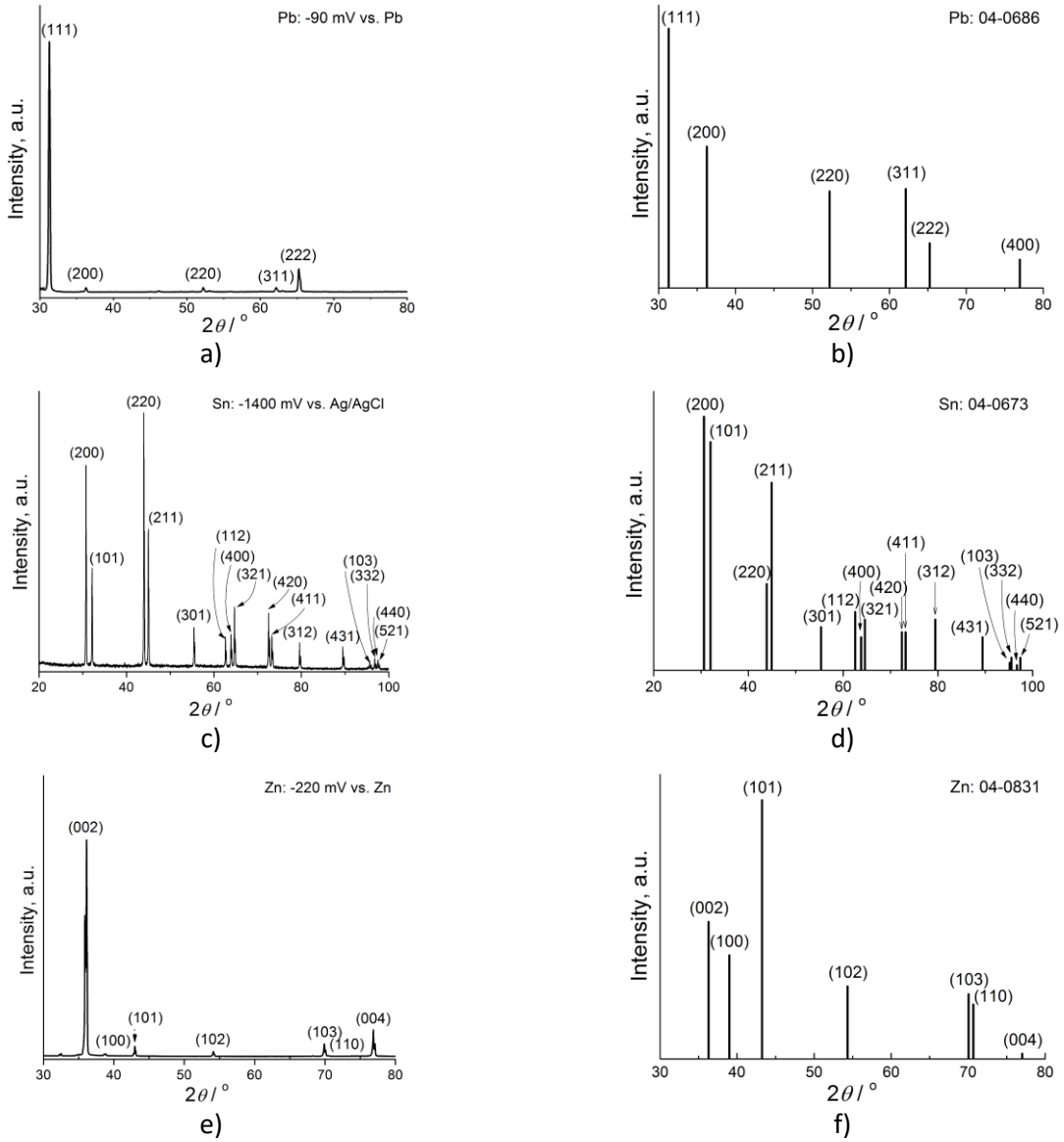

Figure 2. *The XRD patterns and the corresponding standards of (a) and (b) Pb, (c) and (d) Sn, (e) and (f) Zn*

Table 1. *The peak intensity ratios obtained for the particles of Pb, Sn, and Zn and their standards*

	The peak intensity ratios				
	(111) / (200)	(111) / (220)	(111) / (311)	(111) / (222)	(111) / (400)
Pb dendrites	50.1	50.0	50.4	10.6	/
Pb standard	2.00	3.23	3.12	11.1	50.0
	(220) / (200)	(220) / (101)	(220) / (211)	(220) / (301)	(220) / (112)
Sn dendrites	1.25	2.50	1.82	5.85	7.41
Sn standard	0.340	0.378	0.459	2.00	1.48
	(220) / (400)	(220) / (321)	(220) / (420)	(220) / (411)	(220) / (312)
Sn dendrites	6.90	4.00	4.41	7.15	8.92
Sn standard	2.61	1.70	2.27	2.27	1.70
	(220) / (431)	(220) / (103)	(220) / (332)	(220) / (440)	(220) / (521)
Sn dendrites	10.4	49.7	24.1	16.2	21.8
Sn standard	2.62	11.3	6.80	17.0	6.80
	(002)/(100)	(002)/(101)	(002)/(102)	(002)/(103)	(002)/(110)	(002)/(004)
Zn dendrites	66.4	20.6	40.4	33.1	203.4	8.02
Zn standard	1.32	0.530	1.89	2.12	2.52	26.5

(cc) BY

The obtained preferred orientations were in an excellent agreement with those obtained by a quantitative determination by use of a methodology based on a calculation of "Texture Coefficients" and "Relative Texture Coefficients" [23,31,48]. This indicates that the fast estimation of the preferred orientation of the powder particles based on a comparison of the peak intensity ratios is successfully applied and can be used to determine the preferred orientation of the powder particles.

Discussion of the presented results

The 2D fern-like dendrites of various degrees of ramification were obtained by electrolysis of Pb, Sn, and Zn from the corresponding hydroxide electrolytes. As mentioned in the Introduction, all three metals belong to the same group from an electrochemical point of view, *i.e.* to a group of the normal metals. The normal metals are characterized by the high exchange current density values, which means that their electrochemical processes are fast, with the diffusion control attained at relatively low overpotentials [1]. Regardless of the crystal lattice type, Pb, Sn and Zn dendrites exhibited the strong preferred orientation in crystal planes with the lowest surface energy. This clearly indicates that there is a strong correlation between the shape (the 2D fern-like dendrites) and the crystal orientation (the preferred orientation in the crystal plane with the lowest surface energy) of the dendritic particles of Pb, Sn and Zn and that electrochemical parameters (exchange current density values) have a priority over crystallography (belonging to a determined type of crystal lattice).

It can be shown that this strong correlation, which is independent of a type of crystal lattice, has a universal character, *i.e.* is valid for other metals belonging to a group of normal metals. Namely, a strong correlation between morphology and crystal structure is observed in silver, another representative group of normal metals [18]. The 2D fern-like dendrites of silver (the face-centered cubic type of a crystal lattice) electrodeposited from the nitrate electrolyte showed the strong preferred orientation in the (111) crystal plane. Also, it does not depend on the type of electrolyte under which the powder particles are produced. The 2D fern-like Pb dendrites constructed from the trunk and the primary branches electrodeposited from the nitrate electrolyte, as well as those constructed from the trunk, the primary and the secondary branches obtained by electrolysis from the acetate electrolyte exhibited the strong preferred orientation in the crystal plane with the lowest surface energy, *i.e.* in the (111) crystal plane [6]. It is necessary to note that 2D fern-like Pb dendrites obtained from the nitrate electrolyte were very similar to Sn at the macro level (Figure 1c and 1d).

Hence, a degree of ramification of the 2D fern-like dendrites of Pb achieved by the use of various types of electrolytes did not affect the establishment of this correlation. It can also be verified by analysis of the Zn electrolysis process at a higher overpotential than previously reported. Figure 3 shows the morphology of dendrites of Zn electrodeposited at an overpotential of -280 mV *vs.* Zn. Aside from dendrites constructed from a trunk and primary branches (Figure 3a), the appearance of the secondary branches was observed in the Zn dendrites electrodeposited at -280 mV *vs.* Zn (Figure 3b), indicating that a ramification of the dendrites occurred with increasing the overpotential of electrolysis. Finally, the formation of the 3D (three-dimensional) dendrites was also noticed during Zn electrolysis from the hydroxide electrolyte under the given working conditions. These dendrites, formed to a significantly smaller extent than the 2D dendrites, had compact branches oriented in all directions, as shown in Figure 3c.

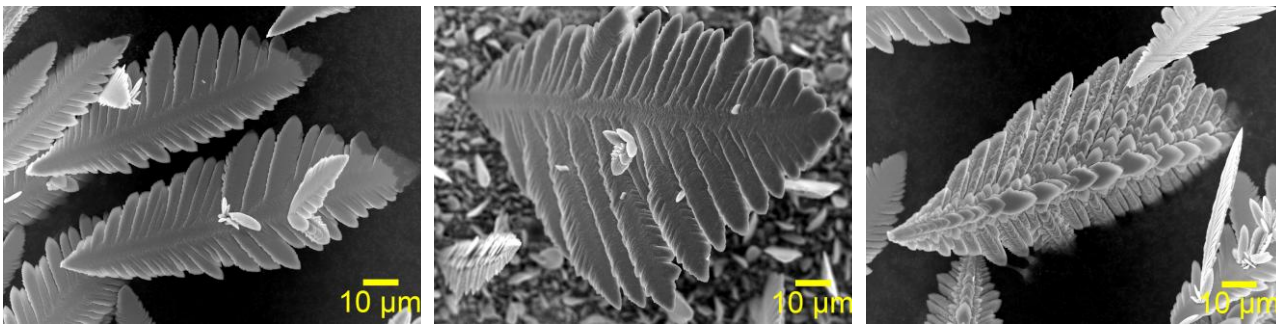

a) b) c)

Figure 3. *The dendrites of Zn obtained by electrolysis at an overpotential of -280 mV vs. Zn: (a) the 2D fern-like dendrites constructed from the trunk and primary branches, (b) the 2D fern-like dendrite constructed from the trunk, primary and secondary branches, and (c) the 3D dendrite*

The XRD pattern of Zn particles produced at an overpotential of -280 mV *vs.* Zn is shown in Figure 4. At first sight, it is clear that it was very similar to that obtained at -220 mV *vs.* Zn. The peak intensity ratios for the given particles are shown in Table 2.

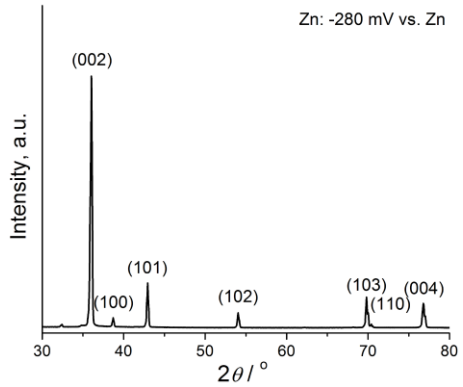

Figure 4. *The XRD pattern of Zn particles electrodeposited at an overpotential of -280 mV vs. Zn*

Table 2. *The peak intensity ratios for Zn dendrites electrodeposited at an overpotential of -280 mV vs. Zn*

	The peak intensity ratios					
	(002)/(100)	(002)/(101)	(002)/(102)	(002)/(103)	(002)/(110)	(002)/(004)
Zn dendrites	22.9	5.52	15.8	8.00	55.2	9.90
Zn standard	1.32	0.530	1.89	2.12	2.52	26.5

Analysis of data given in Table 2 showed that the dendritic particles of Zn showed a strong (002) (004) preferred orientation. The careful analysis of the branches in the 3D dendrites revealed that some of them consisted of hexagons of (002) orientation, additionally contributing to the strong (002) preferred orientation of the dendrites of Zn [48]. The appearance of the 3D dendrites of Zn is understandable because Zn, with the exchange current density values between 18.4 and 88 mA cm^{-2} [5,24], is very close to a boundary between a group of the normal metals and a group of the intermediate metals.

Regardless of the shape of the fern-like dendrites, all of them had a compact structure with no occurrence of spherical grains in them. On the other hand, the approximately spherical grains are the smallest and constitutive unit that build the 3D pine-like dendrites of copper and silver electrodeposited from the ammonium electrolyte [6,18,29]. As already given in the Introduction, Cu and Ag (if electrodeposition is performed from the complex ammonium electrolyte) and gold belong to the group of intermediate metals characterized by lower exchange current density values than the normal metals group. The 3D pine-like dendrites produced via the electrochemical deposition

(cc) BY

route show a random orientation [6,18,29], which is understandable since the standards for estimating the preferred orientation of particles are established for a spherical shape of the grains [42]. This additionally proves the existence of the strong correlation between morphology and crystal orientation of the dendrites, and no matter what Cu and Ag belong to the same group of crystal lattice, it is clear that the electrochemical parameters prevail over the crystallographic affiliation. Nevertheless, the morphology of the 3D dendrites of Zn is completely different from those of the 3D Cu and Ag dendrites.

Conclusions

In this study, a strong correlation between the morphology and the preferred orientation of dendrites of Pb, Sn, and Zn was established. These three metals belong to the group of normal metals characterized by the high values of the exchange current density (the fast electrochemical processes) and electrocrystallize in various kinds of crystal lattice (Pb - the face-centered cubic type, Sn - the body-centered tetragonal type, and Zn - the hexagonal closed pack type). The 2D dendrites of the fern-like shape, with certain differences among themselves in the surface morphology at the macro level, were obtained by electrolysis from the corresponding hydroxide electrolytes.

Applying the procedure based on a comparison of the peak intensity ratios, it was found that the 2D fern-like dendrites of Pb, Sn, and Zn exhibited the strong preferred orientation in a crystal plane with the lowest surface energy, *i.e.* in (111)(222) for Pb, (220)(440) for Sn, and (002)(004) crystal planes for Zn. The strong preferred orientation in the crystal plane with the lowest surface energy observed for various types of crystal lattice and 2D fern-like dendrites confirms a primate of electrochemical parameters (the rate of electrochemical deposition processes, *i.e.* exchange current density values) over crystallography (belonging to a determined type of a crystal lattice).

Acknowledgments: *This research was funded by the Ministry of Science, Technological Development and Innovation of the Republic of Serbia (Contract No. 451-03-66/2024-03/200026).*

References

[1] K. I. Popov, S. S. Djokić, N. D. Nikolić, V. D. Jović, *Morphology of Electrochemically and Chemically Deposited Metals*; Springer, New York, USA, 2016, pp. 1-368. https://doi.org/10.1007/978-3-319-26073-0.

[2] Making Metal Powder, https://www.mpif.org/IntrotoPM/MakingMetalPowder.aspx. (accessed on 04 February 2025)

[3] M. Amiri, S. Nouhi, Y. Azizian-Kalandaragh, Facile synthesis of silver nanostructures by using various deposition potential and time: A nonenzymatic sensors for hydrogen peroxide, *Materials Chemistry and Physics* **155** (2015) 129-135. https://doi.org/10.1016/j.matchemphys.2015.02.009

[4] G. Orhan, G. Hapci, Effect of Electrolysis Parameters on the Morphologies of Copper Powder Obtained in a Rotating Cylinder Electrode Cell, *Powder Technology* **201** (2010) 57-63. https://doi.org/10.1016/j.powtec.2010.03.003

[5] N. D. Nikolić, Influence of the exchange current density and overpotential for hydrogen evolution reaction on the shape of electrolytically produced disperse forms, *Journal of Electrochemical Science and Engineering* **10** (2020) 111-126. https://doi.org/10.5599/jese.707

[6] N. D. Nikolić, V. M. Maksimović, Lj. Avramović, Correlation of Morphology and Crystal Structure of Metal Powders Produced by Electrolysis Processes, *Metals* **11** (2021) 859. https://doi.org/10.3390/met11060859

[7] F. C. Walsh, C. T. J. Low, A review of developments in the electrodeposition of tin, *Surface and Coatings Technology* **288** (2016) 79-94. https://doi.org/10.1016/j.surfcoat.2015.12.081

[8] A. W. Lodge, M. M. Hasan, P. N. Bartlett, R. Beanland, A. L. Hector, R. J. Kashtiban, W. Levason, G. Reid, J. Sloan, D. C. Smith, W. Zhang, Electrodeposition of tin nanowires from a dichloromethane based electrolyte, *RSC Advances* **8** (2018) 24013-24020. https://doi.org/10.1039/C8RA03183E

[9] Z. Wang, J. Ru, Y. Hua, J.Bu, X. Geng, W. Zhang, Electrodeposition of Sn powders with pyramid chain and dendrite structures in deep eutectic solvent: roles of current density and $SnCl_2$ concentration, *Journal of Solid State Electrochemistry* **25** (2021) 1111-1120. https://doi.org/10.1007/s10008-020-04894-7

[10] Z. Wang, J. Ru, Y. Hua, D. Wang, J. Bu, Morphology-Controlled Preparation of Sn Powders by Electrodeposition in Deep Eutectic Solvent as Anodes for Lithium Ion Batteries, *Journal of The Electrochemical Society* **167** (2020) 082504. https://doi.org/10.1149/1945-7111/ab8824

[11] J. Ru, Y. Hua, C. Xu, J. Li, Y. Li, D. Wang, C. Qi, Y. Jie, Morphology-controlled preparation of lead powders by electrodeposition from different PbO-containing choline chloride-urea deep eutectic solvent, *Applied Surface Science* **335** (2015) 153-159. http://dx.doi.org/10.1016/j.apsusc.2015.02.045

[12] J. Ru, J. Bu, Z. Wang, Y. Hua, D. Wang, Eco-friendly and facile electrochemical synthesis of sub-micrometer lead powders in deep eutectic solvents using galena as a raw material, *Journal of Applied Electrochemistry* **49** (2019) 369-377. https://doi.org/10.1007/s10800-018-01284-w

[13] V. S. Cvetković, N. M. Vukićević, N. D. Nikolić, G. Branković, T. S. Barudžija, J. N. Jovićević, Formation of needle-like and honeycomb-like magnesium oxide/hydroxide structures by electrodeposition from magnesium nitrate melts, *Electrochimica Acta* **268** (2018) 494-502. https://doi.org/10.1016/j.electacta.2018.02.121

[14] V. S. Cvetković, N. M. Vukićević, N. D. Nikolić, Z. Baščarević, T. S. Barudžija, J. N. Jovićević, A possible mechanism of formation of flower-like $MgO/Mg(OH)_2$ structures by galvanostatic molten salt electrolysis: The concept of local diffusion fields, *Journal of Electroanalytical Chemistry* **842** (2019) 168-175. https://doi.org/10.1016/j.jelechem.2019.04.067

[15] V. M. Lipkin, L. N. Fesenko, S. M. Lipkin, Tin Powders Electrodeposition from Choline Chloride Based Ionic Liquid, *Solid State Phenomena* **284** (2018) 1252-1256. https://doi.org/10.4028/www.scientific.net/ssp.284.1252

[16] Y. Ni, Y. Zhang, J. Hong, Hierarchical Pb microstructures: a facile electrochemical synthesis, shape evolution and influencing factors, *CrystEngComm* **13** (2011) 934-940. https://doi.org/10.1039/C0CE00272K

[17] R. Sivasubramanian, M. V. Sangaranarayanan, Electrodeposition of silver nanostructures: from polygons to dendrites, *CrystEngComm* **15** (2013) 2052-2056. https://doi.org/10.1039/C3CE26886A

[18] Lj. Avramović, E. R. Ivanović, V. M. Maksimović, M. M. Pavlović, M. Vuković, J. S. Stevanović, N. D. Nikolić, Correlation between Crystal Structure and Morphology of Potentiostatically Electrodeposited Silver Dendritic Nanostructures, *Transactions of Nonferrous Metals Society of China* **28** (2018) 1903-1912. https://doi.org/10.1016/S1003-6326(18)64835-6

[19] M. Yang, W. Xia, J. An, N. Wu, W. Yang, H. Wang, Fractal growth of copper powder on point and plate electrodes based on diffusion-limited aggregation model, *Ionics* **30** (2024) 4313-4323. https://doi.org/10.1007/s11581-024-05554-w

[20] N. Wu, C. Zhang, S. Han, J. An, W. Xia, Effect of Electrolysis Parameters on the Fractal Structure of Electrodeposited Copper, *Journal of Electrochemical Science and Technology* **14** (2023) 194-204. https://doi.org/10.33961/jecst.2022.00878

[21] H.-C. Shin, J. Dong, M. Liu, Nanoporous Structures Prepared by an Electrochemical Deposition Process, *Advanced Materials* **15** (2003) 1610-1614. https://doi.org/10.1002/adma.200305160

(cc) BY

[22] T.-H. Kim, K.-S. Hong, D. R. Sohn, M. J. Kim, D.-H. Nam, E. A. Cho, H. S. Kwon, One-step synthesis of multilayered 2D Sn nanodendrites as a high-performance anode material for Na-ion batteries, *Journal of Materials Chemistry A* **5** (2017) 20304-20315. https://doi.org/10.1039/C7TA06469A
[23] N. D. Nikolić, J. D. Lović, V. M. Maksimović, P .M. Živković, Morphology and structure of electrolytically synthesized tin dendritic nanostructures, *Metals* **12** (2022) 1201. https://doi.org/10.3390/met12071201
[24] N. D. Nikolić, P. M. Živković, J. D. Lović, G. Branković, Application of the general theory of disperse deposits formation in an investigation of mechanism of zinc electrodeposition from the alkaline electrolytes, *Journal of Electroanalytical Chemistry* **785** (2017) 65-74. https://doi.org/10.1016/j.jelechem.2016.12.024
[25] S. J. Banik, R. Akolkar, Suppressing Dendritic Growth during Alkaline Zinc Electrodeposition using Polyethylenimine Additive, *Electrochimica Acta* **179** (2015) 475-481. https://doi.org/10.1016/j.electacta.2014.12.100
[26] J. Rosen, G. S. Hutchings, Q. Lu, R. V. Forest, A. Moore, F. Jiao, Electrodeposited Zn Dendrites with Enhanced CO Selectivity for Electrocatalytic CO_2 Reduction, *ACS Catalysis* **5** (2015) 4586−4591. https://doi.org/10.1021/acscatal.5b00922
[27] P. Lertsathitphong, S. Limpijumnong, M. Somasundrum, A. P. O'Mullane, B. Lertanantawong, Electrochemical Formation of Pb Microwires with Tunable Morphology on Liquid Metal Electrodes, *ACS Omega* **9** (2024) 45641-45650. https://doi.org/10.1021/acsomega.4c09165
[28] V. D. Jović, B. M. Jović, M. G. Pavlović, Electrodeposition of Ni, Co and Ni-Co alloy powders, *Electrochimica Acta* **51** (2006) 5468-5477. https://doi.org/10.1016/j.electacta.2006.02.022
[29] N. D. Nikolić, Lj. Avramović, E. R. Ivanović, V. M. Maksimović, Z. Baščarević, N. Ignjatović, Comparative morphological and crystallographic analysis of copper powders obtained under different electrolysis conditions, *Transactions of Nonferrous Metals Society of China* **29** (2019) 1275-1284. https://doi.org/10.1016/s1003-6326(19)65034-x
[30] D. Desai, X. Wei, D. A. Steingart, S. Banerjee, Electrodeposition of preferentially oriented zinc for flow-assisted alkaline batteries, *Journal of Power Sources* **256** (2014) 145-152. https://doi.org/10.1016/j.jpowsour.2014.01.026
[31] N. D. Nikolić, V. M. Maksimović, G. Branković, P. M. Živković, M. G. Pavlović, Correlation between crystal orientation and morphology of electrolytically produced powder particles: analysis of the limiting cases, *Materials Protection* **59** (2018) 256-264. https://doi.org/10.5937/ZasMat1802256N
[32] D. Perdana, S. Wahyudi, M. Z. Mubarok, Analysis of the Particle Size and Morphology of Tin Powder Synthesized by the Electrolytic Method, *ACS Omega* **9** (2024) 3276-3286. https://doi.org/10.1021/acsomega.3c05179
[33] W. Lou,W. Cai, P. Li, J. Su, S. Zheng, Y. Zhang, W. Jin, Additives-assisted electrodeposition of fine spherical copper powder from sulfuric acid solution, *Powder Technology* **326** (2018) 84-88. https://doi.org/10.1016/j.powtec.2017.12.060
[34] N. D. Nikolić, G. Branković, M. G. Pavlović, Formation of the honeycomb-like electrodes by the regime of pulsating overpotential in the second range, *Journal of Electrochemical Science and Engineering* **2** (2012) 33-40. https://doi.org/10.5599/jese.2012.0009
[35] N. D. Nikolić, G. Branković, M. G. Pavlović, Correlate Between Morphology of Powder Particles Obtained by the Different Regimes of Electrolysis and the Quantity of Evolved Hydrogen, *Powder Technology* **221** (2012) 271-277. https://doi.org/10.1016/j.powtec.2012.01.014
[36] R. K. Nekouei, F. Rashchi, N. N. Joda, Effect of organic additives on synthesis of copper nano powders by pulsing electrolysis, *Powder Technology* **237** (2013) 554-561. https://doi.org/10.1016/j.powtec.2012.12.046

[37] R. Winand, Electrodeposition of metals and alloys - new results and perspectives, *Electrochimica Acta* **39** (1994) 1091-1105. https://doi.org/10.1016/0013-4686(94)E0023-S
[38] C. S. Barrett, T. B. Massalski, *Structure of Metals, Crystallographic Methods, Principles and Data, International Series on Materials Science and Technology*, Pergamon, New York, USA, 1980. ISBN: 008026171X, 9780080261713, pp. 1-654.
[39] X. Zheng, T. Ahmad, W. Chen, Challenges and strategies on Zn electrodeposition for stable Zn-ion batteries, *Energy Storage Materials* **39** (2021) 365-394. https://doi.org/10.1016/j.ensm.2021.04.027
[40] M. N. Kozicki, Information in electrodeposited dendrites, *Advances in Physics: X* **6** (2021) 1920846. https://doi.org/10.1080/23746149.2021.1920846
[41] G. Wranglen, Dendrites and Growth Layers in the Electrocrystallization of Metals, *Electrochimica Acta* **2** (1960) 130-146. https://doi.org/10.1016/0013-4686(60)87010-7
[42] M. V. Mandke, S-H. Han, H. M. Pathan, Growth of silver dendritic nanostructures via electrochemical route, *CrystEngComm* **14** (2012) 86-89. https://doi.org/10.1039/C1CE05791J
[43] J. M. Zhang, F. Ma, K. W. Xu, Calculation of the surface energy of FCC metals with modified embedded-atom method, *Applied Surface Science* **229** (2004) 34-42. https://doi.org/10.1016/j.apsusc.2003.09.050
[44] S. G. Wang, E. K. Tian, C. W. Lung, Surface Energy of Arbitrary Crystal Plane of bcc and fcc Metals, *Journal of Physics and Chemistry of Solids* **61** (2000) 1295-1300. https://doi.org/10.1016/S0022-3697(99)00415-1
[45] H. Fu, L. Xiong, W. Han, M. Wang, Y. J. Kim, X. Li, W. Yang, G. Liu, Highly active crystal planes-oriented texture for reversible high-performance Zn metal batteries, *Energy Storage Materials* **51** (2022) 550-558. https://doi.org/10.1016/j.ensm.2022.06.057
[46] X. Wang, J. P. Meng, X. G. Lin, Y. D. Yang, S. Zhou, Y. P. Wang, A. Q. Pan, Stable zinc metal anodes with textured crystal faces and functional zinc compound coatings, *Advanced Functional Materials* **31** (2021) 2106114. https://doi.org/10.1002/adfm.202106114
[47] J. O.'M. Bockris, A. K. N. Reddy, M. E. Gamboa-Aldeco, *Modern Electrochemistry 2A, Fundamentals of Electrodics*, Springer, New York, USA, 2000, p. 1333 https://doi.org/10.1007/b113922
[48] N. D. Nikolić, J. D. Lović, V. M. Maksimović, N. S. Vuković, N. L. Ignjatović, P. M. Živković, S. I. Stevanović, Correlation Between Morphology and Crystal Structure of Electrolytically Produced Zinc Dendritic Particles, *Metals* **14** (2024) 1468. https://doi.org/10.3390/met14121468

©2025 by the authors; licensee IAPC, Zagreb, Croatia. This article is an open-access article distributed under the terms and conditions of the Creative Commons Attribution license (https://creativecommons.org/licenses/by/4.0/)